

---

# The Role of Global Labels in Few-Shot Classification and How to Infer Them

---

**Ruohan Wang**  
University College London  
ruohan.wang@cs.ucl.ac.uk

**Massimiliano Pontil**  
Istituto Italiano di Tecnologia  
University College London  
massimiliano.pontil@iit.it

**Carlo Ciliberto**  
University College London  
c.ciliberto@ucl.ac.uk

## Abstract

Few-shot learning (FSL) is a central problem in meta-learning, where learners must quickly adapt to new tasks given limited training data. Surprisingly, recent works have outperformed meta-learning methods tailored to FSL by casting it as standard supervised learning to jointly classify all classes shared across tasks. However, this approach violates the standard FSL setting by requiring *global labels* shared across tasks, which are often unavailable in practice. In this paper, we show why solving FSL via standard classification is theoretically advantageous. This motivates us to propose **Meta Label Learning (MeLa)**, a novel algorithm that infers global labels and obtains robust few-shot models via standard classification. Empirically, we demonstrate that MeLa outperforms meta-learning competitors and is comparable to the oracle setting where ground truth labels are given. We provide extensive ablation studies to highlight the key properties of the proposed strategy.

## 1 Introduction

A central problem in machine learning is *few-shot learning* (FSL), where new tasks must be learned quickly given limited training data. A FSL task consists of two datasets: a small support set for model learning, and a query set for evaluating generalization performance. FSL has drawn increasing attention due to the high cost of collecting and annotating large datasets. A significant body of works has tackled FSL using techniques from meta-learning [e.g. 2, 7, 20, 21, 22, 26], which aims to improve generalization in small sample-size settings by leveraging past experiences of solving related tasks. Broadly speaking, meta-learning methods find suitable models by directly learning transferable knowledge over a collection of related FSL tasks.

In this paper, we focus on few-shot classification, the predominant domain in which FSL algorithms are evaluated [see e.g. 2, 4, 25]. Recently, Tian *et al.* have investigated a simple yet highly competitive alternative to meta-learning: a linear model on top of a feature embedding learned via “*global classification*” [24]. This approach ignores task structures from meta-learning and merges all FSL tasks into a “flat” dataset of labeled samples. The desired feature embedding is then learned by classifying all available classes over such a flat dataset. Global classification has been empirically demonstrated to outperform state-of-the-art meta-learning algorithms. In a follow-up, [11] further demonstrated the empirical advantage of global classification by introducing several regularization techniques. Global classification is also widely utilized within meta-learning methods [e.g. 4, 14, 15, 19, 20, 27], either as a pre-processing step to embed input data into a suitable feature representation or as an auxiliary loss to be jointly optimized alongside meta-learning losses.

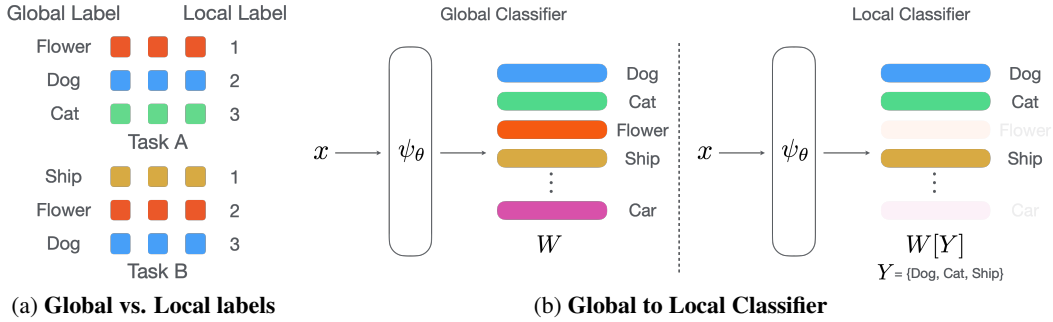


Figure 1: **(a)** Colored squares represent samples. Tasks A and B can be “merged” meaningfully using global labels, but not local ones. Standard FSL has access to local labels only. **(b)** A global classifier can be used as local classifiers given the indices  $Y$  of the intended classes to predict.

Despite the significant empirical improvements, theoretical justifications for applying global classification in FSL are limited: it is unclear why feature embedding learned via global classification performs well as few-shot models. Additionally, global classification requires task merging to construct a flat dataset, which implicitly assumes access to a set of *global labels* consistently adopted across tasks. However, the assumption only holds for benchmark datasets (e.g. *miniIMAGENET* or *CIFAR-FS*) where FSL tasks are synthetically constructed from globally disjoint classes. In contrast, global labels are often unavailable in realistic scenarios, where tasks are independently annotated with *local labels* only. Locally labeled tasks naturally arise in practical applications, when we collate independently annotated datasets to train few-shot models, such as datasets submitted by different users to an automated machine learning service. Standard FSL experiments also adopt independent annotation such that tasks are annotated with local labels 1 through  $K$  for  $K$ -way classification. Fig. 1a illustrates the distinction between global and local labels. Since local labels are only meaningful to individual tasks, direct task merging (see Sec. 2 for more details), as required by global classification, might lead to incoherent labeling of samples across tasks. In the example from Fig. 1a, Label 1 would contain “flower” in Task A and “ship” in Task B after the merge, while Label 2 includes “dog” and “flower”.

In this paper, we address the issues raised above with the following contributions:

- In Sec. 3, we justify the use of global classification in FSL by showing that global classification relates to meta-learning as an upper bound on a meta-learning loss. The connection also suggests several advantages of global classification over existing meta-learning methods.
- In Sec. 4, we propose **Meta Label Learning (MeLa)**, a novel algorithm to infer global labels shared across tasks. The learned labels enable us to leverage global classification for FSL.
- In Sec. 5, we demonstrate empirically that MeLa outperforms state-of-the-art meta-learning methods, and achieve generalization accuracy comparable to the oracle setting where ground truth labels are given as input. We also present an extensive ablation study of the proposed method to highlight its key properties.

Before presenting the contributions above, we recall the key notions of FSL and meta-learning in Sec. 2. The supplementary material accompanying this work contains proofs for the theoretical analysis and additional experiment details.

## 2 Background

In the following, we formalize FSL in the context of meta-learning, followed by the alternative approach of global classification initially investigated in [24].

**Meta-learning.** FSL [6] considers a meta-training set of tasks  $\mathcal{T} = \{(S_t, Q_t)\}_{t=1}^T$ , with *support set*  $S_t = \{(x_j, y_j)\}_{j=1}^{n_s}$  and *query set*  $Q_t = \{(x_j, y_j)\}_{j=1}^{n_q}$  sampled from the same distribution. Typically,  $S_t$  and  $Q_t$  each contains a small number of samples  $n_s$  and  $n_q$  respectively. We denote by  $\mathcal{D}$  the space of datasets of the form  $S_t$  or  $Q_t$ .

FSL aims to find the best base learner  $\text{Alg}(\theta, \cdot) : \mathcal{D} \rightarrow \mathcal{F}$  that maps supports sets  $S$  to predictors  $f = \text{Alg}(\theta, S)$ , such that  $y = f(x)$  generalizes well on the corresponding query sets. The base learner is meta-parametrized by  $\theta \in \Theta$ . Formally, the meta-learning loss for FSL is

$$\min_{\theta \in \Theta} \mathbb{E}_{(S,Q) \in \mathcal{T}} \mathcal{L}(\text{Alg}(\theta, S), Q), \quad (1)$$

where  $\mathbb{E}_{(S,Q) \in \mathcal{T}} \triangleq \frac{1}{|\mathcal{T}|} \sum_{(S,Q) \in \mathcal{T}}$  denotes the empirical distribution over the meta-training set. The task loss  $\mathcal{L} : \mathcal{F} \times \mathcal{D} \rightarrow \mathbb{R}$  is the empirical risk of the learner over query sets, according to an inner loss  $\ell$ ,

$$\mathcal{L}(f, D) = \mathbb{E}_{(x,y) \in D} [\ell(f(x), y)]. \quad (2)$$

Various base learners  $\text{Alg}(\theta, \cdot)$  have been proposed in the literature. We focus on the formulation of meta-representation learning [2, 9, 16], which has been observed to be remarkably effective in practice and is closely related to the global classification strategy to be discussed next. Meta-representation learning considers a base learner in an embedded space,

$$\mathbb{E}_{(S,Q) \in \mathcal{T}} [\mathcal{L}(w(\psi_\theta(S)), \psi_\theta(Q))] \quad (3)$$

where  $\psi_\theta : \mathcal{X} \rightarrow \mathbb{R}^m$  is a feature embedding model and  $\psi_\theta(D) \triangleq \{(\psi_\theta(x), y) | (x, y) \in D\}$  the embedded dataset. In [2], the base learner  $\text{Alg}(\theta, D) = w(\psi_\theta(D))$  is defined as ridge regression

$$w(D) = \underset{W}{\text{argmin}} \mathbb{E}_{(x,y) \in D} [\|Wx - \text{OneHot}(y)\|^2 + \lambda_1 \|W\|^2], \quad (4)$$

where  $\lambda_1$  is a constant. Among different base learners, ridge regression is often favored for its differentiable closed-form solution and the associated computational efficiency in optimizing (3).

**Global Classification.** We now review the global classification strategy considered in [24]. Given the meta-training set  $\mathcal{T}$ , a “flat” dataset  $D_{\text{global}}$  is constructed by merging all tasks in  $\mathcal{T}$ :

$$D_{\text{global}} = D(\mathcal{T}) = \{(x_i, y_i)\}_{i=1}^N = \bigcup_{(S,Q) \in \mathcal{T}} (S \cup Q). \quad (5)$$

We then learn the embedding function  $\psi_\theta$  on  $D_{\text{global}}$  using the standard cross-entropy loss  $\ell_{\text{ce}}$  for multi-class classification:

$$\underset{\theta, W}{\text{argmin}} \mathbb{E}_{(x,y) \in D_{\text{global}}} [\ell_{\text{ce}}(W\psi_\theta(x), y)]. \quad (6)$$

After obtaining  $\psi_\theta$ , a novel task may be tackled using a base learner similar to (4) in the embedded space. In [24], the authors observed that the regularized logistic regression estimator

$$w_{\text{ce}}(D) = \underset{W}{\text{argmin}} \mathcal{L}_{\text{ce}}(W, D) + \lambda_2 \|W\|^2, \quad (7)$$

consistently yielded the best empirical performance. Here  $\lambda_2$  is a regularization constant. We note that ridge regression is no longer favored as a base learner here since optimizing (6) is independent of base learner choices.

We refer to the above strategy as *global classification* since  $\psi_\theta$  is trained to jointly classify all available classes from meta-training set  $\mathcal{T}$ . Global classification has demonstrated state-of-the-art test accuracy in FSL [11, 24], outperforming many meta-learning methods tailored for FSL. In Sec. 3, we contribute a theoretical justification for using global classification in FSL (when possible to do so, see below). In particular, we show that global classification relates to an upper bound on the meta-learning loss. This connection also suggests several advantages of global classification, including improved performance over existing meta-learning methods.

**Global vs. Local Labels.** Crucially, the prerequisite for applying global classification is the feasibility of task merging. This operation is meaningful only if  $y_i$  in (5) are “global” labels shared across tasks. However, global labels may be unavailable when each task is annotated independently, a realistic scenario detailed in Sec. 1. In fact, most implementations of FSL experiments assume independent annotation: each task is assigned local labels from 1 through  $K$  for  $K$ -way classification. See Fig. 1a for an illustration of this issue. Independent annotation captures wide-ranging scenarios in which direct task merging is challenging, including nondescript classes (e.g. tasks with numerical labels) or concept overlaps between classes across tasks (e.g. sea animals vs. mammals). In Sec. 4, we propose a novel algorithm that infers global labels across tasks, thus eliminating them from required input.

### 3 Global Classification as Meta-learning

In this section, we show how global classification relates to meta-learning as a loss upper bound. More precisely, we show that the meta-learning loss is upper bounded by the cross-entropy loss from global classification. As a result, minimizing the cross-entropy loss indirectly minimizes the meta-learning loss, hence finding a model also suitable for FSL. Further, we compare the meta-learning loss induced by global classification against standard meta-learning losses (e.g. Eq. (3)), and highlight several advantages related to global classification.

Let  $\mathcal{T} = \{(S_t, Q_t)\}_{t=1}^T$  be a meta-training set *where all tasks are annotated with global labels*. We denote the collection of query sets as  $\mathcal{Q} = \{Q_t\}_{t=1}^T = \{(X_t, Y_t)\}_{t=1}^T$  where we write  $Q_t = (X_t, Y_t)$  as a tuple of input samples  $X_t = \{x_{jt}\}_{j=1}^{n_q}$  and their corresponding labels  $Y_t = \{y_{jt}\}_{j=1}^{n_q}$ . For simplicity, we assume that the query sets are disjoint, namely  $Q_t \cap Q_{t'} = \emptyset$  for any  $t \neq t'$ . We merge all query sets into a flat dataset  $D(\mathcal{Q}) = \{(x_i, y_i)\}_{i=1}^N = \cup_{t=1}^T Q_t$ , with  $N = n_q T$ .

**Proposition 1.** *With the notation and assumptions introduced above, let  $C$  be the total number of classes in  $D(\mathcal{Q})$ , and  $W \in \mathbb{R}^{C \times m}$  the global classifier. Denote by  $W[Y]$  the sub-matrix with rows indexed by the sorted unique values<sup>1</sup> from  $Y$ . Then, for any embedding  $\psi_\theta : \mathcal{X} \rightarrow \mathbb{R}^m$*

$$\mathbb{E}_{(X,Y) \in \mathcal{Q}} \left[ \mathcal{L}_{\text{ce}}(W[Y], (\psi_\theta(X), Y)) \right] \leq \mathbb{E}_{(x,y) \in D(\mathcal{Q})} [\ell_{\text{ce}}(W\psi_\theta(x), y)], \quad (8)$$

We outline the proof strategy here and defer the details to the supplementary material. We first observe that  $D(\mathcal{Q})$  has the same collection of samples as  $\mathcal{Q}$ . Secondly, each matrix  $W[Y]$  is in fact a local classifier for the query set  $(X, Y)$ . Crucially, the likelihood of query samples  $p(Y|X)$ , estimated by local classifiers  $W[Y]$ , are no smaller than their likelihood estimated by the global classifier  $W$ , which forms the inequality in (8). Combining the two observations yields Prop. 1.

The key implication of Prop. 1 is that, *when global labels are available*, we can use a special base learner

$$w_{\text{global}}(D) = w_{\text{global}}(X, Y) = W[Y], \quad (9)$$

for any dataset of the form  $D = (X, Y)$ . This base learner relies only on the intended classes to predict (i.e. unique values in  $Y$ ) and is independent of any specific samples from  $D$ . The proposition thus suggests a straightforward strategy to find local classifiers: train a global classifier  $W$  by minimizing the right-hand side of (8) and then, when tackling a new task with labels  $Y$ , simply use the corresponding rows  $W[Y]$  as described in Prop. 1 (also see Fig. 1b). We note that for any task  $(S, Q) \in \mathcal{T}$ ,  $w_{\text{global}}(S) = w_{\text{global}}(Q)$ , since the support and query sets share the same class labels. These observations directly imply the following result.

**Lemma 2.** *For meta-training set  $\mathcal{T}$  where tasks are annotated with global labels, we have*

$$\mathbb{E}_{(S,Q) \in \mathcal{T}} \left[ \mathcal{L}_{\text{ce}}(w_{\text{global}}(S), \psi_\theta(Q)) \right] = \mathbb{E}_{(X,Y) \in \mathcal{Q}} \left[ \mathcal{L}_{\text{ce}}(W[Y], (\psi_\theta(X), Y)) \right]. \quad (10)$$

Note that the left-hand side of (10) corresponds to (1), the meta-learning objective for FSL. Hence, the combination of Prop. 1 and Lemma 2 implies that the empirical risk associated with the meta-learning loss is upper bounded by the standard cross-entropy loss, namely the right-hand side of (8). The connection justifies the use of global classification for FSL (when global labels are available) since minimizing the cross-entropy loss indirectly minimizes the meta-learning loss. In particular, the embedding function  $\psi_\theta$  is shared between both sides of (8), which implies that learning  $\psi_\theta$  via global classification is equivalent to meta-representation learning from (3). Empirically,  $\psi_\theta$  is known to work well with different base learners [4, 24], in addition to the one being optimized for. This allows us to replace (9) with (7) to handle novel classes during meta-testing.

**Remark 1.** *The bound in Prop. 1 is tight when the standard cross-entropy loss is 0.*

Remark 1 shows that all local classifiers  $W[Y]$  and the embedding function  $\psi_\theta$  are optimal, when standard cross-entropy is 0. In practice, Remark 1 is achievable since over-parametrized neural networks could obtain zero empirical loss.

Eq. (10) in fact describes a conditional meta-learning problem [5, 27], where global labels  $Y$  provide additional side information to facilitate learning. Apart from their intended purpose of

<sup>1</sup>E.g.  $Y = \{6, 6, 4, 9\}$  maps to  $\{4, 6, 9\}$ -th rows of  $W$ . Also see Fig. 1b for an illustration.

---

**Algorithm 1** MeLa

---

**Input:** meta-training set  $\mathcal{T} = \{S_i, Q_i\}_{i=1}^T$   
 $\psi_\theta^0 = \operatorname{argmin}_{\psi_\theta} \mathbb{E}_{(S,Q) \in \mathcal{T}} [\mathcal{L}(w(\psi_\theta(S)), \psi_\theta(Q))]$   
Global clusters  $G = \operatorname{LearnLabeler}(\psi_\theta^0, \mathcal{T})$   
 $\psi_\theta^* = \operatorname{GlobalClassify}(G, \mathcal{T})$   
**Return**  $\psi_\theta^*$

---

classifying samples within a task, global labels also directly reveal how a task relates to all other tasks. Consequently, the base learner  $w_{\text{global}}$  could simply map global labels to task classifiers, leveraging the global classifier  $W$ . In contrast, unconditional base learners (e.g. Eq. (4) and (7)) learn classifiers based on support sets, ignoring any task relations provided by global labels. In [5], the authors have shown theoretically that conditional meta-learning is advantageous over unconditional meta-learning by incurring a smaller excess risk. This could explain why global classification yields a more robust  $\psi_\theta$  compared to many meta-learning methods and leads to better test accuracy. We refer the readers to [5] for further discussion on conditional meta-learning.

Global classification also has other practical advantages. Since  $w_{\text{global}}$  only depends on global labels, the embedding function  $\psi_\theta$  learned via global classification is suitable for arbitrary support sets, regardless of the number of samples or classes in them. In other words, a single embedding  $\psi_\theta$  learned via global classification is suitable for all  $K$ -way- $P$ -shots settings found in FSL. Lastly, global classification is typically more computationally efficient than meta-learning, without having to optimize with respect to base learners.

## 4 Meta Label Learning

In Sec. 3, we have justified the use of global classification in FSL and highlighted its advantages, including improved performance and computational efficiency. However, access to global labels may be unavailable in practical applications, rendering many methods unusable. In the following, we address the problem of automatically inferring global labels across tasks, which enables us to apply global classification in FSL.

Alg. 1 outlines our proposed strategy. We first meta-learn an embedding function  $\psi_\theta^0$  as a tool to measure sample similarity. Secondly, we introduce a novel algorithm for clustering samples across tasks and use the resulting clusters as global labels. Lastly, we apply global classification using the inferred labels to obtain the desired few-shot model  $\psi_\theta^*$ . Since Phase 1 and 3 are standard procedures, we only detail the algorithm for inferring labels below.

The labeling algorithm takes a meta-training set as input and outputs a set of clusters to represent global labels. The algorithm consists of a clustering step for updating centroids and a pruning step for merging small clusters. The algorithm is presented in Alg. 2.

**Clustering Step.** The procedure exploits local labels from each task to guide sample assignments. For each task, local labels are used to enforce two constraints: samples with the same local label should be assigned the same global label, while samples from different local classes should be assigned different global ones. Formally, given a set of cluster centroids  $G = \{g_j\}_{j=1}^J$ , we assign all samples  $\{x_i\}_{i=1}^I$  sharing the same local label within a task to a single global cluster by a weighted voting mechanism,

$$v^* = \operatorname{argmin}_v \frac{1}{I} \sum_{i=1}^I \|\psi_\theta^0(x_i) - g_v\|^2. \quad (11)$$

We apply (11) to each class of samples in a task, matching  $K$  clusters in total. For simplicity, we discard tasks in which multiple local classes map to the same cluster. Otherwise, we update each matched cluster  $g_{v^*}$  and sample counts  $N_{v^*}$  with

$$g_{v^*} = \frac{N_{v^*} g_{v^*} + \sum_{i=1}^I (\psi_\theta^0(x_i))}{N_{v^*} + I} \quad \text{and} \quad N_{v^*} = N_{v^*} + I, \quad (12)$$

**Pruning Step.** We present a simple pruning strategy to regulate the number of clusters. Under the mild assumption that each cluster is equally likely to appear in a task, a cluster  $v$  is sampled with

---

**Algorithm 2** LearnLabeler

---

**Input:** embedding model  $\psi_\theta^0$ , meta-training set  $\mathcal{T} = \{S_t, Q_t\}_{t=1}^T$ , number of classes in a task  $K$

**Initialization:** sample tasks from  $\mathcal{T}$  to initialize clusters  $G = \{g_j\}_{j=1}^J$ ,

```
while  $|G|$  has not converged do
   $N_v = 1$  for each  $g_v \in G$ 
  for  $(S, Q) \in \mathcal{T}$  do
     $(X, Y) = S \cup Q$  //use both support and query set
    Match global clusters  $V = \{v_q\}_{q=1}^K$  via (11) for task  $(X, Y)$ 
    if  $V$  has  $K$  unique clusters then
      Update cluster  $v$  for each  $v \in V$  via (12)
    end if
  end for
  Compute threshold via (13)
   $G \leftarrow \{g_v | g_v \in G, N_v \geq \text{threshold}\}$ 
end while
Return  $S$ 
```

---

probability  $p = \frac{K}{J}$  for each  $K$ -way classification task. The number of samples  $N_v$  assigned to cluster  $v$  thus follows a binomial distribution with  $N_v \propto B(T, p)$  where we recall  $T$  as the size of the meta-training set. We remove any cluster below the threshold

$$N_v < \bar{N}_v - q\sqrt{\text{Var}(N_v)} \quad (13)$$

where  $\bar{N}_v$  is the mean of  $N_v$ ,  $\text{Var}(N_v)$  the variance, and  $q$  a hyper-parameter controlling the aggressiveness of the pruning process.

Alg. 2 initializes a large number of clusters and populates the centroids with mean class embeddings computed from random tasks in  $\mathcal{T}$ . For  $J$  initial clusters,  $\lceil \frac{J}{K} \rceil$  tasks are needed since each task contributes  $K$  embeddings. The algorithm alternates between clustering and pruning to refine the centroids and estimate the number of clusters. When the number of existing clusters no longer changes, the algorithm terminates and returns the current centroids  $G$ .

Alg. 2 differs from the classical  $K$ -mean algorithm [10] in several ways. The proposed algorithm does not need prior knowledge about the number of global labels for the meta-training set. Instead, the algorithm initialize a large number of clusters (e.g. 3000 for *tiered*IMAGENET) and automatically estimates the number of clusters via hyperparameter  $q$  in (13), which can be interpreted as the number of standard deviations from the mean. In addition, Alg. 2 exploits local information to guide the clustering process, while  $K$ -mean algorithm is fully unsupervised. We will show experimentally that 1) the labeling algorithm is robust to a wide range of  $q$ , and 2) enforcing local constraints is necessary for learning robust models.

Given the clusters  $G$ , all samples from the meta-training set can be assigned global labels. Each local class of samples in a task is mapped to a single cluster via (11). Global classification is then performed using the learned labels to obtain the desired few-shot model  $\psi_\theta^*$ .

**Connection with Self-Supervised Learning.** The proposed algorithm obtains the embedding function via inferring global labels. Alternatively, embedding functions may be directly learned without labels, using self-supervised learning [e.g. 1, 3, 8, 23]. For instance, MoCo [8] and CMC [23] are able to learn embedding functions based on instance-discrimination. A critical difference between MeLa and self-supervised methods is that they are not designed to leverage any information from the local labels. We compare against the two methods in the experiments.

## 5 Experiments

We evaluate our proposed method on two standard benchmarks, *mini*IMAGENET [26] and *tiered*IMAGENET [18]. As discussed in Sec. 3, global classification allows us to learn a single embedding  $\psi_\theta^*$  for both 5-way-1-shot and 5-way-5-shot settings. All experiments adopts independent annotation with local labels 1 through 5 for 5-way classification. Model details, hyperparameter values and experiment code are included in the supplementary material.



Table 1: Classification accuracy of meta-learning models on *mini*IMAGENET and *tiered*IMAGENET. †: official implementation re-evaluated without data augmentation (see text for more information).

	Accuracy (%)			
	<i>mini</i> IMAGENET		<i>tiered</i> IMAGENET	
	1-shot	5-shot	1-shot	5-shot
Local Labels				
MAML [7]	48.7 ± 1.8	63.1 ± 0.9	51.7 ± 1.8	70.3 ± 0.8
Reptile [13]	49.9 ± 0.3	66.0 ± 0.6	-	-
ProtoNet [22]	49.4 ± 0.8	68.2 ± 0.7	53.3 ± 0.9	72.7 ± 0.7
R2D2 [2]	51.9 ± 0.2	68.7 ± 0.2	-	-
CAVIA [28]	51.8 ± 0.7	65.8 ± 0.5	-	-
MetaOptNet [9]†	56.6 ± 0.6	74.1 ± 0.5	62.3 ± 0.7	80.1 ± 0.6
Shot-free [17]	59.0 ± n/a	<b>77.6</b> ± n/a	63.5 ± n/a	82.6 ± n/a
Initial Embedding (Eq. (3))	59.9 ± 0.3	75.3 ± 0.5	64.3 ± 0.5	78.9 ± 0.4
MeLa (Ours)	<b>60.2 ± 0.4</b>	<b>77.6 ± 0.3</b>	<b>69.0 ± 0.5</b>	<b>84.1 ± 0.3</b>
Global Labels				
SNAIL [12]	55.7 ± 1.0	68.9 ± 0.9	-	-
TADAM [14]	58.5 ± 0.3	76.7 ± 0.3	-	-
LEO [20]†	<b>60.3 ± 0.7</b>	75.4 ± 0.4	65.1 ± 0.7	79.7 ± 0.6
Oracle [24]†	<b>60.2 ± 0.4</b>	<b>77.6 ± 0.3</b>	<b>69.6 ± 0.4</b>	<b>84.4 ± 0.3</b>
No Labels (Self-Supervised)				
MoCo [8]	54.2 ± 0.9	73.0 ± 0.6	-	-
CMC [23]	56.1 ± 0.9	73.9 ± 0.7	-	-

## 5.1 Experiments on ImageNet Variants

We compare MeLa to a representative set of meta-learning algorithms. We split the compared methods based on whether they require global labels as input. The comparison also avoids input augmentation since most augmentation techniques are specific to image tasks and may be less applicable to other domains. Further, we include [24] as the oracle setting of the proposed algorithm. We also include comparison with self-supervised methods for completeness. Tab. 1 reports the average accuracy of the different methods.

In the “local labels” setting, MeLa outperforms the baselines in three out of four settings, and obtains performance comparable to [17] in the remaining one. We highlight the comparison between the initial embedding  $\psi_\theta^0$  obtained via (3) and the final embedding  $\psi_\theta^*$  obtained by MeLa as they share identical experimental setups. It is thus easy to attribute the performance improvements to the proposed algorithm of label learning followed by global classification. In particular, MeLa improves the average test performance by more than 4% in *tiered*IMAGENET.

As discussed in Sec. 3 and [17], we wish to stress that access to global labels divides FSL into two distinct settings that may not be directly comparable, since global labels provide additional side information unavailable to other methods. Nevertheless, MeLa achieves performance comparable to the oracle, and outperforms other baselines in the “global labels” setting. The comparison with the oracle indicates the efficacy of the proposed labeling algorithm.

Tab. 1 also indicates that MeLa outperforms two state-of-the-art self-supervised methods. These results are not surprising given that self-supervised methods are not designed to leverage any label information to facilitate learning.

## 5.2 Impact of Pruning Threshold

In Alg. 2, the pruning threshold is controlled by the hyper-parameter  $q$ . We investigate how different  $q$  values affect the number of clusters estimated by the labeling algorithm and the corresponding test accuracy.

Table 2: The effects of pruning threshold on test accuracy and the number of clusters.

<i>mini</i> IMAGENET (64 classes)				<i>tiered</i> IMAGENET (351 classes)			
$q$	No. Clusters	1-shot(%)	5-shot(%)	$q$	No. Clusters	1-shot(%)	5-shot(%)
4.5	58	59.6 $\pm$ 0.5	76.8 $\pm$ 0.4	4	363	69.0 $\pm$ 0.5	84.1 $\pm$ 0.3
5.5	58	59.6 $\pm$ 0.5	76.8 $\pm$ 0.4	4.5	427	68.5 $\pm$ 0.4	83.6 $\pm$ 0.3
6.5	64	60.2 $\pm$ 0.4	77.6 $\pm$ 0.3	5.5	752	68.4 $\pm$ 0.4	83.5 $\pm$ 0.3

The results suggest that MeLa is robust to a wide range of  $q$  and obtains similar performance for different  $q$  values. With appropriate  $q$  values, the number of clusters estimated for the two datasets are very close to the actual number of global classes. For *mini*IMAGENET, the labeling algorithm could recover exactly 64 classes. While it is possible to replace  $q$  with directly guessing the number of clusters in Alg. 2, we note that tuning for  $q$  is much more convenient since appropriate  $q$  values appear to concentrate within a much narrower range, compared to the possible numbers of clusters.

### 5.3 Robustness of the Labeling Algorithm

A potentially trivial solution for clustering samples without any learning is by looking for identical samples: an identical sample appearing in multiple tasks would allow several local classes to be assigned to the same cluster. To demonstrate that Alg. 2 is not trivially matching identical samples across task, we introduce a more challenging evaluation setting: each sample only appears once in the meta-training set. This implementation constructs the meta-training set by sampling from a flat dataset *without replacement*<sup>2</sup>. Consequently, Alg. 2 must rely on the initial embedding function  $\psi_{\theta}^0$  for estimating sample similarity. We evaluate MeLa under this setting and report the results in Tab. 3.

Table 3: The effects of initial embedding function on the labeling algorithm

Dataset Replacement	<i>mini</i> IMAGENET		<i>tiered</i> IMAGENET	
	Yes	No	Yes	No
Percentage of Tasks Clustered (%)	100	98.6	99.9	89.5
Clustering Acc (%)	100	99.3	96.4	96.4
1-shot Acc (%)	60.2 $\pm$ 0.4	60.2 $\pm$ 0.5	69.0 $\pm$ 0.5	69.0 $\pm$ 0.5
5-shot Acc (%)	77.6 $\pm$ 0.3	77.5 $\pm$ 0.4	84.1 $\pm$ 0.3	84.0 $\pm$ 0.3

In Tab. 3, clustering accuracy is computed by assigning the most frequent ground truth label in each cluster as the desired target. In addition, percentage of tasks clustered refers to the tasks that map to  $K$  unique clusters by Alg. 2. The clustered tasks satisfy the constraints imposed by local labels and are used for global classification.

The results suggest that Alg. 2 is robust in inferring accurate global labels, even when samples do not repeat across tasks. The no-replacement setting also has negligible impact on test performance. In particular, we note that *mini*IMAGENET is particularly challenging under the new setting, with only 384 tasks in the meta-training set. In contrast, the typical sample-with-replacement setting has access to an exponential number of tasks for training.

### 5.4 The Importance of Local Constraints

As discussed in Sec. 4, the clustering process enforces consistent assignment of task samples based on their local labels. To understand the importance of enforcing these constraints, we consider an ablation study where Alg. 2 is replaced with standard  $K$ -mean algorithm, while Phase 1 and 3 of MeLa remain unchanged.  $K$ -mean algorithm is fully unsupervised and ignores any local constraints. We initialize the  $K$ -mean algorithm with 64 clusters for *mini*IMAGENET and 351 clusters for *tiered*IMAGENET, the actual numbers of classes in respective datasets. The results are reported in Tab. 4.

The results indicate that enforcing local constraints is critical in accurately inferring the global labels, as measured by clustering accuracy. In addition, lower clustering accuracy directly translates

<sup>2</sup>The setting implies that *mini*IMAGENET (38400 training samples) can be split into 384 tasks of 100 samples. *tiered*IMAGENET can be similarly split into about 4480 tasks.



Table 4: Comparison between Alg. 2 and  $K$ -mean Clustering

Cluster Alg.	Clustering Acc (%)	Meta-Test Set		Meta-Train Set	
		1-shot	5-shot	1-shot	5-shot
<i>mini</i> IMAGENET					
Alg. 2 (MeLa)	100	$60.2 \pm 0.4$	$77.6 \pm 0.3$	$95.1 \pm 0.2$	$99.5 \pm 0.1$
$K$ -mean	84.9	$59.7 \pm 0.5$	$76.6 \pm 0.3$	$89.1 \pm 0.4$	$96.3 \pm 0.2$
<i>tiered</i> IMAGENET					
Alg. 2 (MeLa)	96.4	$69.0 \pm 0.5$	$84.1 \pm 0.3$	$87.3 \pm 0.4$	$95.5 \pm 0.2$
$K$ -mean	28.2	$63.9 \pm 0.6$	$78.5 \pm 0.5$	$76.1 \pm 0.6$	$87.5 \pm 0.4$

to lower test accuracy during meta-testing, suggesting that sensible task merging is an important prerequisite for applying global classification. In particular, test accuracy drops by over 5% when *tiered*IMAGENET is poorly clustered with  $K$ -mean algorithm. Moreover, poor clustering also worsens the classification accuracy on tasks from the meta-training set. This is relevant since test tasks in practical applications could easily share global labels with the meta-training set.

Between the two local constraints, we note that (11) is more important for accurately inferring global labels. Specifically, the clustering step improves accuracy by averaging the votes from all samples sharing the same local label in a task. On the other hand, the constraint on matching  $K$  unique clusters has minimal impact on clustering accuracy since almost all tasks could be matched to  $K$  clusters under the regular sample-with-replacement setting (see Tab. 3).

## 6 Discussion

Recent works on meta-learning have observed that global classification significantly improves the test performance in FSL [e.g. 4, 14, 20, 24]. In this paper, we show that global classification closely relates to meta-learning as a loss upper bound. In particular, global classification induces a conditional meta-learning problem, which has been shown to incur small excess risk in recent theoretical work [5] and thus improve model performance. The connection between meta-learning and global classification opens up many opportunities of directly applying existing techniques from supervised learning towards FSL. For instance, model distillation [24] and label mix-up [11] has been shown to further improve the performance of few-shot models obtainable from global classification. Both techniques are immediately applicable to MeLa, but not to standard meta-learning methods.

We proposed a practical algorithm to infer global labels, which are necessary for applying global classification. We demonstrate that our algorithm is robust and accurate in inferring global labels, and achieves test performance comparable to the oracle setting. The proposed method also outperforms existing meta-learning methods.

The ablation experiments revealed interesting properties about meta-learning models. We observed that meta-learning methods implicitly learn to cluster samples across tasks, even when samples do not repeat. However, the initial meta-representation is not ideal, and explicitly enforcing the local constraints is critical for accurately inferring global labels and learning robust few-shot models.

**Limitations and Future Work.** We close by discussing some limitations of our work and directions of future research. In this paper, we focused on understanding the connection between global classification and meta-learning, and evaluated MeLa on standard benchmarks that have globally disjoint classes. It is unclear if the current method scales to more diverse and realistic scenarios, when labels across tasks exhibit more complex relationships. For instance, Meta-Dataset [25] is a collection of independently annotated datasets where class labels could be overlapping or exhibit hierarchical relationships. We intend to extend our method to such settings in future works. One possible approach is to assign soft labels or multiple labels to samples, thus capturing more complex relationship between classes.

## References

- [1] Y. M. Asano, C. Rupprecht, and A. Vedaldi. Self-labelling via simultaneous clustering and representation learning. *International Conference on Learning Representations*, 2020.
- [2] L. Bertinetto, J. F. Henriques, P. H. Torr, and A. Vedaldi. Meta-learning with differentiable closed-form solvers. *International conference on learning representations*, 2019.
- [3] M. Caron, P. Bojanowski, A. Joulin, and M. Douze. Deep clustering for unsupervised learning of visual features. In *Proceedings of the European Conference on Computer Vision (ECCV)*, pages 132–149, 2018.
- [4] W.-Y. Chen, Y.-C. Liu, Z. Kira, Y.-C. F. Wang, and J.-B. Huang. A closer look at few-shot classification. In *International Conference on Learning Representations*, 2018.
- [5] G. Denevi, M. Pontil, and C. Ciliberto. The advantage of conditional meta-learning for biased regularization and fine-tuning. In *Advances in Neural Information Processing Systems*, 2020.
- [6] L. Fei-Fei, R. Fergus, and P. Perona. One-shot learning of object categories. *IEEE transactions on pattern analysis and machine intelligence*, 28(4), 2006.
- [7] C. Finn, P. Abbeel, and S. Levine. Model-agnostic meta-learning for fast adaptation of deep networks. In *Proceedings of the 34th International Conference on Machine Learning-Volume 70*. JMLR. org, 2017.
- [8] K. He, H. Fan, Y. Wu, S. Xie, and R. Girshick. Momentum contrast for unsupervised visual representation learning. In *Proceedings of the IEEE/CVF Conference on Computer Vision and Pattern Recognition*, pages 9729–9738, 2020.
- [9] K. Lee, S. Maji, A. Ravichandran, and S. Soatto. Meta-learning with differentiable convex optimization. In *Proceedings of the IEEE/CVF Conference on Computer Vision and Pattern Recognition*, pages 10657–10665, 2019.
- [10] S. Lloyd. Least squares quantization in pcm. *IEEE transactions on information theory*, 28(2): 129–137, 1982.
- [11] P. Mangla, N. Kumari, A. Sinha, M. Singh, B. Krishnamurthy, and V. N. Balasubramanian. Charting the right manifold: Manifold mixup for few-shot learning. In *Proceedings of the IEEE/CVF Winter Conference on Applications of Computer Vision*, pages 2218–2227, 2020.
- [12] N. Mishra, M. Rohaninejad, X. Chen, and P. Abbeel. A simple neural attentive meta-learner. *arXiv preprint arXiv:1707.03141*, 2017.
- [13] A. Nichol, J. Achiam, and J. Schulman. On first-order meta-learning algorithms. *arXiv preprint arXiv:1803.02999*, 2018.
- [14] B. Oreshkin, P. R. López, and A. Lacoste. Tadam: Task dependent adaptive metric for improved few-shot learning. In *Advances in Neural Information Processing Systems*, pages 721–731, 2018.
- [15] S. Qiao, C. Liu, W. Shen, and A. L. Yuille. Few-shot image recognition by predicting parameters from activations. In *Proceedings of the IEEE Conference on Computer Vision and Pattern Recognition*, pages 7229–7238, 2018.
- [16] A. Raghu, M. Raghu, S. Bengio, and O. Vinyals. Rapid learning or feature reuse? towards understanding the effectiveness of maml. *arXiv preprint arXiv:1909.09157*, 2019.
- [17] A. Ravichandran, R. Bhotika, and S. Soatto. Few-shot learning with embedded class models and shot-free meta training. In *Proceedings of the IEEE/CVF International Conference on Computer Vision*, pages 331–339, 2019.
- [18] M. Ren, E. Triantafillou, S. Ravi, J. Snell, K. Swersky, J. B. Tenenbaum, H. Larochelle, and R. S. Zemel. Meta-learning for semi-supervised few-shot classification. *International conference on learning representations*, 2018.
- [19] P. Rodríguez, I. Laradji, A. Drouin, and A. Lacoste. Embedding propagation: Smoother manifold for few-shot classification. In *European Conference on Computer Vision*, pages 121–138. Springer, 2020.
- [20] A. A. Rusu, D. Rao, J. Sygnowski, O. Vinyals, R. Pascanu, S. Osindero, and R. Hadsell. Meta-learning with latent embedding optimization. *International conference on learning representations*, 2019.

- [21] A. Santoro, S. Bartunov, M. Botvinick, D. Wierstra, and T. Lillicrap. Meta-learning with memory-augmented neural networks. In *International conference on machine learning*, 2016.
- [22] J. Snell, K. Swersky, and R. Zemel. Prototypical networks for few-shot learning. In *Advances in Neural Information Processing Systems*, pages 4077–4087, 2017.
- [23] Y. Tian, D. Krishnan, and P. Isola. Contrastive multiview coding. *arXiv preprint arXiv:1906.05849*, 2019.
- [24] Y. Tian, Y. Wang, D. Krishnan, J. B. Tenenbaum, and P. Isola. Rethinking few-shot image classification: a good embedding is all you need? *European Conference on Computer Vision*, 2020.
- [25] E. Triantafillou, T. Zhu, V. Dumoulin, P. Lamblin, U. Evci, K. Xu, R. Goroshin, C. Gelada, K. Swersky, P.-A. Manzagol, and H. Larochelle. Meta-dataset: A dataset of datasets for learning to learn from few examples. In *International Conference on Learning Representations*, 2019.
- [26] O. Vinyals, C. Blundell, T. Lillicrap, D. Wierstra, et al. Matching networks for one shot learning. In *Advances in neural information processing systems*, 2016.
- [27] R. Wang, Y. Demiris, and C. Ciliberto. Structured prediction for conditional meta-learning. *Advances in Neural Information Processing Systems*, 2020.
- [28] L. M. Zintgraf, K. Shiarlis, V. Kurin, K. Hofmann, and S. Whiteson. Fast context adaptation via meta-learning. In *Proceedings of the 36th International Conference on Machine Learning-Volume 70*. JMLR. org, 2019.

# Supplementary Material: The Role of Global Labels in Few-Shot Classification and How to Infer Them

The supplementary material is organized as follows:

- Appendix A contains the proofs accompanying our theoretical analysis.
- Appendix B presents additional experiment results.
- Appendix C details experimental setups, model architecture and hyperparameter values.

## A Proofs

Let  $\mathcal{T} = \{(S_t, Q_t)\}_{t=1}^T$  be a meta-training set where all tasks are annotated with global labels. We denote the collection of query sets as  $\mathcal{Q} = \{Q_t\}_{t=1}^T = \{(X_t, Y_t)\}_{t=1}^T$  where we write  $Q_t = (X_t, Y_t)$  as a tuple of query input samples  $X_t = \{x_{jt}\}_{j=1}^{n_q}$  and their corresponding labels  $Y_t = \{y_{jt}\}_{j=1}^{n_q}$ . For simplicity, we assume that the query sets are disjoint, namely  $Q_t \cap Q_{t'} = \emptyset$  for any  $t \neq t'$ . We merge all query sets into a flat dataset  $D(\mathcal{Q}) = \{(x_i, y_i)\}_{i=1}^N = \cup_{t=1}^T Q_t$ , with  $N = n_q T$ .

**Proposition A.1.** *With the notation and assumptions introduced above, let  $C$  be the total number of classes in  $D(\mathcal{Q})$ , and  $W \in \mathbb{R}^{C \times m}$  the global classifier. Denote by  $W[Y]$  the sub-matrix with rows indexed by the sorted unique values from  $Y$ . Then, for any embedding  $\psi_\theta : \mathcal{X} \rightarrow \mathbb{R}^m$*

$$\mathbb{E}_{(X,Y) \in \mathcal{Q}} [\mathcal{L}_{\text{ce}}(W[Y], (\psi_\theta(X), Y))] \leq \mathbb{E}_{(x,y) \in D(\mathcal{Q})} [\ell_{\text{ce}}(W\psi_\theta(x), y)], \quad (\text{A.1})$$

*Proof.* For a dataset  $D$ , let  $\pi(D)$  be the set of class labels from  $D$ .

$$\mathbb{E}_{(x,y) \in D} [\ell_{\text{ce}}(W\psi_\theta(x), y)] = \frac{1}{N} \sum_{(x,y) \in D} -\log \frac{\exp(W[y]\psi_\theta(x))}{\sum_{y' \in \pi(D(\mathcal{Q}))} \exp(W[y']\psi_\theta(x))} \quad (\text{A.2})$$

$$= \frac{1}{N} \sum_{Q \in \mathcal{Q}} \sum_{(x,y) \in Q} -\log \frac{\exp(W[y]\psi_\theta(x))}{\sum_{y' \in \pi(D(\mathcal{Q}))} \exp(W[y']\psi_\theta(x))} \quad (\text{A.3})$$

(A.3) rewrites the cross-entropy loss by enumerating over  $\mathcal{Q}$ . We observe that  $\mathcal{Q}$  and  $D(\mathcal{Q})$  share the same collection of samples, since all query sets are disjoint.

$$(\text{A.3}) \geq \frac{1}{T} \sum_{Q \in \mathcal{Q}} \frac{1}{n_q} \sum_{(x,y) \in Q} -\log \frac{\exp(W[y]\psi_\theta(x))}{\sum_{y' \in \pi(Q)} \exp(W[y']\psi_\theta(x))} \quad (\text{A.4})$$

$$= \frac{1}{T} \sum_{(X,Y) \in \mathcal{Q}} [\mathcal{L}_{\text{ce}}(W[Y], (\psi_\theta(X), Y))] \quad (\text{A.5})$$

$$= \mathbb{E}_{(X,Y) \in \mathcal{Q}} [\mathcal{L}_{\text{ce}}(W[Y], (\psi_\theta(X), Y))] \quad (\text{A.6})$$

In (A.4), the inequality is formed because the denominator  $\sum_{y' \in \pi(D(\mathcal{Q}))} \exp(W[y']^\top \psi_\theta(x))$  is replaced with smaller values by summing over a smaller number of classes from  $\pi(Q)$ . Lastly, we rewrites the equation as the expectation over tasks in  $\mathcal{Q}$ .

Taking (A.2) and (A.6) yields

$$\mathbb{E}_{(X,Y) \in \mathcal{Q}} [\mathcal{L}_{\text{ce}}(W[Y], (\psi_\theta(X), Y))] \leq \mathbb{E}_{(x,y) \in D(\mathcal{Q})} [\ell_{\text{ce}}(W\psi_\theta(x), y)] \quad (\text{A.7})$$

□

**Remark A.1.** *If  $\mathbb{E}_{(x,y) \in D(\mathcal{Q})} [\ell_{\text{ce}}(W\psi_\theta(x), y)] = 0$ ,*

$$\mathbb{E}_{(X,Y) \in \mathcal{Q}} [\mathcal{L}_{\text{ce}}(W[Y], (\psi_\theta(X), Y))] = \mathbb{E}_{(x,y) \in D(\mathcal{Q})} [\ell_{\text{ce}}(W\psi_\theta(x), y)] = 0.$$

*Proof.* If  $\mathbb{E}_{(x,y) \in D(\mathcal{Q})} [\ell_{ce}(W\psi_{\theta}(x), y)] = 0$ , By Proposition 1,

$$\mathbb{E}_{(X,Y) \in \mathcal{Q}} [\mathcal{L}_{ce}(W[Y], (\psi_{\theta}(X), Y))] \leq 0$$

As cross-entropy loss  $\mathcal{L}_{ce}(\cdot) \geq 0$ , we have  $\mathbb{E}_{(X,Y) \in \mathcal{Q}} [\mathcal{L}_{ce}(W[Y], (\psi_{\theta}(X), Y))] = 0$   $\square$

## B Additional Experiment On CIFAR Variants

In this section we present additional experiments on CIFAR-FS and CIFAR-100 datasets.

The CIFAR-FS dataset [2] is derived from the original CIFAR-100 dataset by randomly splitting 100 classes into 64, 16 and 20 classes for training, validation, and testing, respectively. The FC100 dataset [14] is also constructed from CIFAR-100 dataset with the classes split in a way similar to *tiered*IMAGENET. The exact splits used in our experiments are identical to [24].

We evaluate MeLa on both CIFAR-FS and FC100 in 5-way-1-shot and 5-way-5-shot settings. The results are reported in Table 5.

Table 5: Comparison on CIFAR-FS and FC100 benchmarks

	Accuracy (%)			
	CIFAR-FS		FC100	
	1-shot	5-shot	1-shot	5-shot
MAML [7]	58.9 ± 1.9	71.5 ± 1.0	-	-
R2D2 [2]	65.3 ± 0.2	79.4 ± 0.1	-	-
TADAM [14]	-	-	40.1 ± 0.4	56.1 ± 0.4
Shot-free [17]	69.2 ± n/a	84.7 ± n/a	-	-
ProtoNet [22]	72.2 ± 0.7	83.5 ± 0.5	37.5 ± 0.6	52.5 ± 0.6
MetaOptNet [9]	<b>72.6 ± 0.7</b>	84.3 ± 0.5	41.1 ± 0.6	55.5 ± 0.6
MeLa (Ours)	71.4 ± 0.5	<b>85.6 ± 0.4</b>	<b>44.0 ± 0.5</b>	<b>59.5 ± 0.5</b>
Oracle [24]	71.6 ± 0.5	<b>85.7 ± 0.4</b>	<b>44.4 ± 0.5</b>	<b>60.0 ± 0.5</b>

Table 5 suggests that MeLa obtains test performance comparable to the oracle setting. This further validates that global labels may not be necessary as input, and that our proposed labeling algorithm is effective in inferring meaningful global labels across tasks. In addition, MeLa outperforms other meta-learning baselines in 3 out of 4 settings, and is only slightly worse than MetaOptNet in the remaining setting. While the high-dimensional embedding used by MetaOptNet (16000 dimensions vs 640 in ours) may be advantageous for some scenarios (e.g. CIFAR-FS 1-shot setting), they are potentially difficult to scale to larger tasks and global classification still produces more robust embedding overall. Lastly, we note that the test performance obtainable by global classification could be further improved via model distillation, as demonstrated in [24]. We expect MeLa to obtain similar performance gains from distillation, since it is able to recover the ground truth labels and the number of classes with high accuracy for both CIFAR-FS and FC100.

## C Model and Experimental Setups

We provide additional details on the model architecture, experiment setups, and hyperparameter choices. We performed only limited model tuning, as it is not the focus on the work.

### C.1 Model Architecture

We use a ResNet-12 architecture for all our experiments. The architecture strikes a good balance between model complexity and performance, and is one of the most commonly adopted architecture in existing works [e.g. 9, 14, 17, 24]. Specifically, we adopt the default architecture from the official implementation<sup>3</sup> of [24]. The model’s penultimate layer is averaged and outputs an embedding  $\psi_{\theta}(x) \in \mathbb{R}^{640}$ .

<sup>3</sup><https://github.com/WangYueFt/rfs>

## C.2 Experiment Setup

For each dataset, we train a single  $\psi_\theta^*$  for both 1-shot and 5-shot settings. The initial embedding function  $\psi_\theta^0$  can be trained on either 1-shot or 5-shot setting with minimal impact on the quality of  $\psi_\theta^*$ . We choose the latter in our experiments. To ensure fair comparison, we follow the existing convention and use 15 samples per class for query sets  $Q$ .

For all experiments, we adopt an initial learning rate of 0.05. The learning rate is decayed by a factor of 0.1 twice for all datasets. All models are trained using a SGD optimizer with a momentum of 0.9 and a weight decay of  $5 \times 10^{-4}$ .

Table 6 reports hyperparameter values used in our experiments. Datasets CIFAR-FS and FC100 share the same values and are reported under ‘‘CIFAR’’.

Table 6: Hyperparameter values used in the experiments

SYMBOL	DESCRIPTION	VALUES		
		<i>mini</i> IMAGENET	<i>tiered</i> IMAGENET	CIFAR
$\lambda_1$ IN (4)	REGULARIZER FOR RIDGE REGRESSION	$10^{-3}$	$10^{-3}$	$10^{-3}$
$\lambda_2$ IN (7)	REGULARIZER FOR LOGISTIC REGRESSION	1	1	1
$J$	INITIAL NUMBER OF CLUSTERS	300	3000	300
$q$	PRUNING PARAMETER IN (13)	6.5	4.5	4.5

## C.3 Meta-Testing

For all of our models, we use

$$w_{ce}(Z) = \operatorname{argmin}_W \mathcal{L}_{ce}(W, Z) + \lambda_2 \|W\|^2 \tag{C.1}$$

as the base learner for meta-testing. (C.1) is implemented by scikit-learn<sup>4</sup> and identical to the one used in [24]. We observe empirically that this base learner outperforms other common choices such as ProtoNet [22] or SVM [9].

## C.4 Computational Requirements

All experiments are runnable on a commodity desktop PC with a single Nvidia 2080 Ti and 48GB of RAM. MeLa takes about 3 hours to train for *mini*IMAGENET and about 6 hours to train for *tiered*IMAGENET. CIFAR-FS and FC100 both take about 1.5 hours for training.

<sup>4</sup><https://scikit-learn.org/stable/>